

Benchmarking graph construction by large language models for coherence-driven inference

Steve Huntsman
and Jewell Thomas

STEVE.HUNTSMAN@CYNNOVATIVE.COM
JEWELL.THOMAS@CYNNOVATIVE.COM

Abstract

We devise an algorithm to generate propositions that objectively instantiate graphs supporting coherence-driven inference. We also benchmark the ability of large language models (LLMs) to reconstruct coherence graphs from (a simple transformation of) propositions expressed in natural language, with promising results from a single prompt to reasoning-optimized LLMs. For example, `o1/3/4-mini` achieve perfect reconstruction half of the time on sparse graphs. Coherence-driven inference on consistency evaluations by LLMs may advance machine cognition capabilities.

1. Introduction

Classical *coherence-driven inference* (CDI) (Thagard and Verbeurgt, 1998; Thagard, 2002; Blokpoel and van Rooij, 2024) models many forms of cognition as solving a constraint satisfaction problem. In this approach, propositions and their consistency relations are encoded in a weighted graph G as in Figures 1, 2, and 3. Up to an irrelevant constant that varies among formulations, the *coherence* of $U \subseteq V(G)$ is $-\sum_{u \in U, v \notin U} A_{uv}$, where $V(G)$ is the vertex set of G and A is the weighted adjacency matrix of G . (As is common in the literature, we often assume $A_{uv} \in \{\pm 1\}$ in this paper; our benchmarking approach handles this case naturally.) The problem of maximizing coherence is thus an instance for the matrix $-A$ of the APX-complete MAX-CUT problem (Khot et al., 2007; Moore and Mertens, 2011; Gärtner and Matousek, 2012; Lee and Xu, 2021). The objective is to cut the most negative weights in G with a bipartition into accepted (= estimated true) and rejected (= estimated false) propositions.^{1 2}

CDI is deeply informed by cognitive science, and experimentally validated by psychological case studies, including assessments of legal reasoning (Holyoak and Simon, 1999; Simon, 2004). It is a computationally credible model for causal inference (Thagard, 2004) suited for making decisions about ill-structured problems (Frigotto and Rossi, 2015). Other illustrations of its capacity for high-level reasoning include reaching deliberative consensus (Joseph and Prakken, 2009), solving normative inconsistencies (Criado et al., 2016), and many complementary examples cited in Blokpoel and van Rooij (2024). CDI can also explicitly incorporate ethical considerations and

1. Near-optimal *Rashomon* solutions (Semenova et al., 2022) can become optimal if the graph is perturbed. CDI can account for these by averaging over a Gibbs measure for coherence to indicate probabilities of acceptance.

2. In general, context matters for assigning acceptance and rejection to a computed bipartition. The most common approach is to prioritize data. For example, direct observations and firm prior conclusions carry more weight than secondhand reports and tentative prior conclusions. See Blokpoel and van Rooij (2024) for a discussion of this point and remarks about implementing a data priority scheme in the present context. (Implementing a data priority scheme is straightforward in the more general computational context outlined in §A.2: just introduce appropriately weighted [or “hard”] single-variable clauses into a weighted SAT instance.) A natural criterion *in vacuo* is to prioritize the part of the bipartition whose induced subgraph has greater normalized internal coherence.

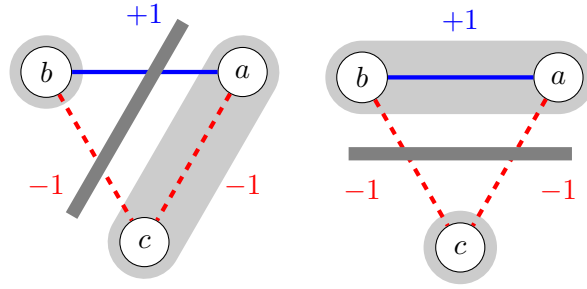


Figure 1: Left: the coherence graph G associated with the propositions $a : X$ is hot, $b : X$ is bright, and $c : X$ is cold and dark. Consistent (solid blue) and inconsistent (red dashed) pairs of vertices (= propositions) respectively get positive and negative weights. Also shown is the cut $\{\{a, c\}, \{b\}\}$ whose coherence is $-(A_{ab} + A_{bc}) = -((+1) + (-1)) = 0$, where A is the weighted adjacency matrix of G . Right: the associated coherence graph G with the cut $\{\{a, b\}, \{c\}\}$ whose coherence is $-(A_{ac} + A_{bc}) = -((-1) + (-1)) = 2$. CDI amounts to accepting and rejecting data according to a cut $\{U, V(G) - U\}$ that maximizes the coherence objective $-\sum_{u \in U, v \notin U} A_{uv}$. The cut on the right is optimal, separating propositions according to their inconsistencies.

Athenians

- $p1$: The strong dominate and the weak endure.
- $p2$: Internal rebellion is a greater threat to Athens than external rivals like Lacedaemon.
- $p3$: Subjugating Melos would strengthen Athenian security and expand the Athenian empire.
- $p4$: Melian neutrality would show Athenian weakness.
- $p5$: Hope is risky and unreliable, especially for those with few resources like the Melians.
- $p6$: Both gods and men support ruling wherever possible.
- $p7$: The Lacedaemonians prioritize security and are unlikely to intervene in support of Melos.

Melians

- $p8$: Justice and fairness protect weaker states like Melos.
- $p9$: Athenian aggression risks creating more enemies for Athens and alienating neutral states.
- $p10$: Resisting Athens is about honor and survival for the Melians.
- $p11$: War's unpredictability offers hope to the Melians against stronger foes like Athens.
- $p12$: The gods and the Lacedaemonians will support Melos due to justice and kinship with the Melians.

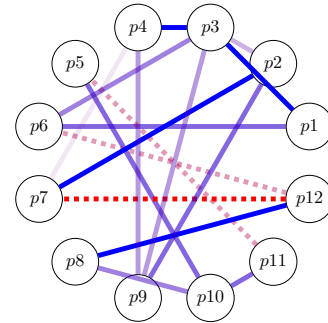


Figure 2: Left: The 12 most important propositions in the Melian Dialogue from Thucydides (1874) as extracted and processed by GPT-4o. (NB. Lacedaemon is an ancient name for Sparta.) Right: The median of 30 coherence graphs produced by single prompts to o1-mini along the lines of §J. Convergence of the median coherence graph is illustrated in §H. Consistent (solid blue) and inconsistent (red dashed) pairs of vertices (= propositions) respectively get positive and negative weights, with intermediate colors and transparency indicating the strength of (in)consistency. The optimal cut has parts $\{p1, p2, p3, p4, p6, p7, p9\}$ and $\{p5, p8, p10, p11, p12\}$. Note that $p5$ and $p9$ “cross the line” between Athens and Melos in opposite directions: their significance is highlighted in history. A hopeful Melos was brutally conquered by Athens in 416 BCE, during a truce with Sparta. Sparta later defeated Athens in the Peloponnesian War in 405 BCE, removed Athenians from Melos, and resettled surviving Melians there.

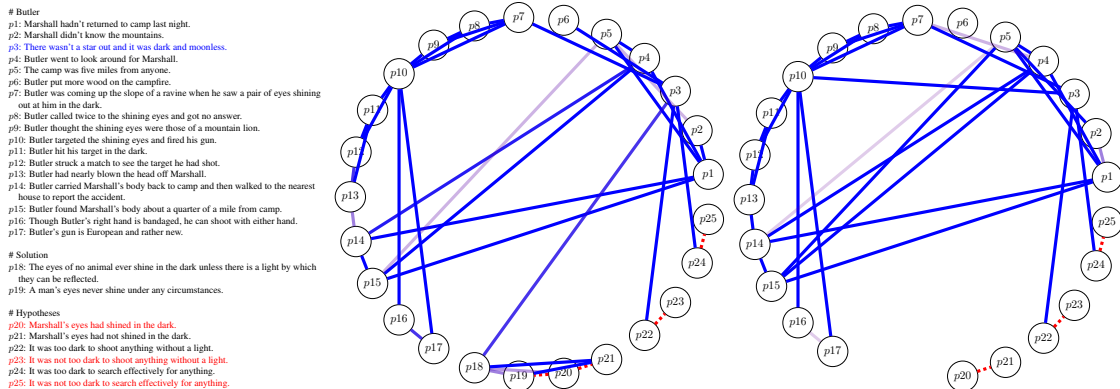


Figure 3: Left: Propositions adapted from the first mystery in Ripley (1932), along with its solution and six relevant hypotheses. Center: The median of 30 coherence graphs produced by single prompts to `o1-mini`. Right: The result of omitting solution data from prompts. In each median graph an optimal cut **accepts the key observation p_3** and **rejects hypotheses p_{20} , p_{23} , and p_{25}** that are inconsistent with the solution explaining Butler’s guilt.

provide explanations of its reasoning (Yilmaz et al., 2017; Sivaraj and Yilmaz, 2019). However, mechanisms for automatically generating coherence graphs from natural language have not been developed: coherence graphs have almost always been constructed manually. (A notable exception is the specialized construction of Joseph and Prakken (2009) with deduction from underlying logic.)

In this paper, we show how to generate a set of propositions expressible in natural language that objectively instantiate a given signed coherence graph. We then use this result to benchmark the ability of large language models (LLMs) (Brown et al., 2020) to (re)construct signed coherence graphs, with promising results from a single prompt to models optimized for reasoning: see Figures 6-8 and §D. Given a “correct” coherence graph, the CDI process amounts to running a MAX-CUT solver or analogue thereof, along with conceptually straightforward ancillary tasks. Viewed in this light, our work demonstrates the initial feasibility for a neurosymbolic architecture (Sarker et al., 2022; Marra et al., 2024) that combines neural reasoning by an LLM to compile a coherence graph with symbolic reasoning via CDI to reason over the graph. This architecture naturally separates concerns and is unique in the breadth of straightforward applications.

In particular, CDI is suited for “slow” or “system 2” reasoning with hard computations performed on impoverished representations (Kahneman, 2011). In contrast, previous neurosymbolic efforts that use LLMs to help with graph coloring (Khandelwal et al., 2024) or transform natural language data into a logical formula to be passed to a solver (Olausson et al., 2023; Pan et al., 2023; Ye et al., 2024) reason at a low level of abstraction, cannot resolve ambiguity after the representational process, and can suffer from parsing errors (Feng et al., 2024). Meanwhile, benchmarks appropriate for evaluating the performance of such efforts using propositional or first-order logic (Zhong et al., 2021; Han et al., 2022; Saparov and He, 2023) are not suitable for evaluating coherence.

Meanwhile, transformer-based architectures (Vaswani et al., 2017) like LLMs are suited for “fast” or “system 1” reasoning with easy computations on rich representations (Lenat and Marcus, 2023; Bengio and Malkin, 2024). Transformers are computationally weak without chain-of-thought (CoT) reasoning, but become more powerful with it (Merrill and Sabharwal, 2024). In principle,

using CoT linear in input size allows transformers to simulate automata and recognize regular languages, or emulate a probabilistic Turing machine in quasi-quadratic time (Pérez et al., 2021; Nowak et al., 2024). Transformers using polynomial-size CoT can also solve the problems in \mathbf{P} . However, the computation of a transformer with L layers on a prompt of length n can be performed using $O(L \log n)$ bits of memory under common assumptions. As a corollary, multilayer transformers cannot scalably solve the easy problems 2-SAT or Horn-SAT unless $\mathbf{L} = \mathbf{NL}$ (Peng et al., 2024). On the other hand, the representational power of multi-head transformer architectures is bounded below by n -gram models (Rajaraman et al., 2024), which perform well in practice (Liu et al., 2024).

Besides its clean separation of neural and symbolic reasoning, a key advantage and enabler of our approach is that an LLM takes independent and identically distributed samples from some distribution over coherence graphs. Our results show that even individual coherence graphs can be reconstructed with excellent precision and recall. There is a simple explanation for this. Asking an LLM to attempt to logically *interpolate* between pairs of propositions and characterize this process with a numerical rating is more tightly constrained, and therefore less prone to hallucinations and their ilk, than *extrapolating* responses from open-ended prompts. Taking a median of the individual realizations almost inevitably yields robust coherence graphs. This procedure amounts to optimal consensus in the sense of graph edit distance and an optimal rank one approximation in the L^1 norm of the matrix whose columns are vectorized weighted adjacency matrices. Furthermore, resampling and taking medians yields a quantitative measure of robustness.

Observations on realistic examples such as Figure 2—for which convergence is shown in §H—and Figure 3 (for which convergence is not shown, but similar) indicate that the median L^1 /graph edit distance between medians of n out of $N = 30$ responses to prompts generally decreases rapidly to near zero as a function of n . (The decrease is slower in more complex examples such as poker hands. Sharp, late decreases appear to indicate topological “phase transitions” in global connectivity that require more capable models or other scaling fixes.) Moreover, while several median coherence graphs generated for (e.g.) Figures 2 and 3 exhibited some residual variation, our experiments suggest that these generally share an optimal cut (not detailed here, but see the right panel of Figure 3). It is therefore plausible that individual coherence graph realizations are sparse approximations that approximately preserve all of the cuts of a denser, implicit “Platonic” (hyper)graph (Benczúr and Karger, 1996; Spielman and Teng, 2011; Soma and Yoshida, 2019). If this is indeed the case, it could explain connectivity transitions as due to hyperedges being sparsified in uniformly different ways, so that resulting edges vanish when taking a median over a large enough sample.

Our approach holds promise for autonomy that is explainable (by analyzing [near-] optimal cuts); ethical (by including ethical guidelines as data (Yilmaz et al., 2017; Sivaraj and Yilmaz, 2019)); reproducible and stable (see, e.g., Figure 3 and §H); versatile (by using any sufficiently capable multimodal or domain-specific model); intrinsically capable of handling abstraction and ambiguity; grounded in a flexible cognitive model; and generalizable by construction (see §A.2).

The examples we provide are already at scales commensurate with hand-crafted coherence graphs in the literature. As such, the scalability of our approach for many if not most practical purposes is governed by the ability to organize and compose smaller inferences into larger inferences. This amounts to promoting (only) relevant accepted propositions from one instance of inference to the next, whether hierarchically or sequentially. Scaling to “simply” larger coherence graphs to achieve more human (or superhuman) cognitive abilities is of questionable utility in light of a fixed-parameter tractable cognition hypothesis articulated in Van Rooij (2008); Van Rooij et al. (2019).

The paper is organized as follows. §2 explains how to produce propositions that naturally correspond to a given coherence graph. §3 outlines our experimental setup and §4 details the most important results of our experiments. We conclude in §5. Appendices respectively give substantial information on generalizing and computing CDI (§A); a case study in which ChatGPT 4 outperformed a skilled human at assigning consistency ratings to proposition pairs (§B); ANOVA (§C); modeling and reconstructing under uncertainty (§D); the effects of using different graph-theoretical algorithms in our benchmarking approach (§E); a preliminary mechanistic interpretation of how attention mechanisms may underlie our results (§F); characteristics of the graphs we generated for benchmarking (§G); an example of how median consensus coherence graphs converge (§H); our prompt templates (§I and §J), and finally an alternative fidelity characterization (§K).

We plan to release code and data in the coming weeks.

2. Modeling coherence graphs

Here we describe how to benchmark classical CDI using signed graphs, which approximate more elaborate constructions such as weighted simplicial complexes that may be appropriate for modeling and computing coherence in full generality (for which see Huntsman et al. (2024) and §A.2).

Definition 1 Recall that a signed graph $G_\sigma = (V, E, \sigma)$ is an undirected graph $G = (V, E)$ augmented with a sign map $\sigma : E \rightarrow \{\pm 1\}$. A signed coherence graph is a signed graph whose vertices are propositions.³ Two propositions v and w are dependent in G_σ if $(v, w) \in E$ (in particular, v and w are assumed to be distinct). Two dependent propositions are consistent for σ (resp., inconsistent for σ) if $\sigma(v, w) = +1$ (resp., -1). The left panel of Figure 4 shows an example.

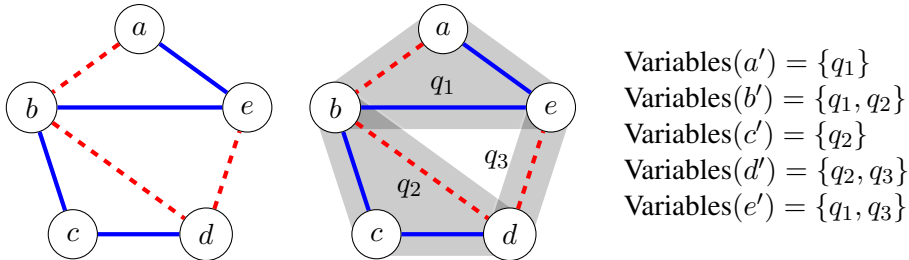


Figure 4: Left: a signed coherence graph for propositions $\{a, \dots, e\}$, with consistent pairs (a, e) , (b, c) , (b, e) , and (c, d) indicated by solid blue edges, corresponding to edge weights of $+1$; and inconsistent pairs (a, b) , (b, d) , and (d, e) indicated by dashed red edges, corresponding to edge weights of -1 . Center: cliques q_1 , q_2 , and q_3 (indicated by gray vertex clusters) yield a minimal clique edge partition (hence cover). Right: each vertex is assigned variables corresponding to the cliques that cover it.

A consistency oracle ε is a function that sends any pair of distinct propositions expressed in natural language to $\{-1, 0, 1\}$. When $\varepsilon(v, w) = -1, 0$, and 1 , v and w are respectively (dependent and) inconsistent for ε , independent for ε , and (dependent and) consistent for ε . While LLMs can

3. In practice we can use a more expressive framework than (natural language generation applied to) propositional logic, but we use the term *proposition* throughout; Algorithm 1 involves *bona fide* propositional formulas.

effectively detect inconsistencies between two propositions (see [Huntsman et al. \(2024\)](#); [Kumar and Roussinov \(2024\)](#), and §B), we will initially restrict consideration to synthetic propositions for which the output of any “reasonable” consistency oracle (i.e., one in which propositions that express logical formulas in natural language are evaluated in the natural way suggested by the underlying formulas) is practically obvious and unambiguous.

Definition 2 *Given a consistency oracle ε , a signed coherence graph $G_\sigma = (V, E, \sigma)$, a set of propositions V' expressed in natural language, and a bijection $\iota : V' \rightarrow V$, we say that V' models G_σ relative to ε and write $V' \models_\varepsilon G_\sigma$ if for all distinct $v', w' \in V'$ we have $\varepsilon(v', w') = \sigma_0(\iota(v'), \iota(w'))$, where σ_0 extends σ by the value 0 on pairs of independent distinct propositions.*

We will give a general method for constructing $V' \models_\varepsilon G_\sigma$ under any reasonable consistency oracle ε , which we informally write $V' \models G_\sigma$.

For example, taking G_σ to be the signed coherence graph in the left panel of Figure 4,

$$V' = \{a' : (q_1 \text{ is } p_1), \quad b' : (q_1 \text{ is NOT } p_1 \text{ AND } q_2 \text{ is NOT } p_1), \quad c' : (q_2 \text{ is } p_2), \\ d' : (q_2 \text{ is } p_1 \text{ AND } q_3 \text{ is } p_1), \quad e' : (q_1 \text{ is } p_2 \text{ AND } q_3 \text{ is NOT } p_1)\}$$

where the (*clique*) variables q_j are placeholders for nouns and the (*properties*) p_k are placeholders for gradable (hence negatable) adjectives (e.g., “hot,” “bright,” “loud,” etc.) and $\iota : a' \mapsto a, \dots, e' \mapsto e$, we can see that $V' \models G_\sigma$. A structurally equivalent model $V'' \models G_\sigma$ is

$$V'' = \{a'' : (\text{the living room is hot}), \quad b'' : (\text{the living room is cold and the kitchen is cold}), \\ c'' : (\text{the kitchen is bright}), \quad d'' : (\text{the kitchen is hot and the bedroom is hot}), \\ e'' : (\text{the living room is bright and the bedroom is cold})\}.$$

While there are structurally inequivalent sets of propositions that model G_σ , a set of the form above is extremal in that its clique edge cover and star forest decomposition are minimal: see §2.1.

2.1. An algorithm for modeling signed coherence graphs

Here we detail how to construct a set of propositions that model a signed coherence graph.

Definition 3 *A clique edge cover of a graph G ([Erdős et al., 1966](#); [Gross et al., 2018](#); [Conte et al., 2020](#)) is a set of cliques in G whose edges cover $E(G)$. A star forest decomposition of G ([Akiyama and Kano, 1985](#); [Kottarathil et al., 2024](#)) is a partition of $E(G)$ into star forests, i.e., forests whose connected components each have only a single vertex of degree greater than 1: see Figure 5.*

Note that the sizes of clique edge covers and star forest decompositions are saturated below by the *intersection number* and *star arboricity*, respectively.

Theorem 4 *Given a signed coherence graph $G_\sigma = (V, E, \sigma)$, Algorithm 1 produces $V' \models G_\sigma$.*

Proof It suffices to show that $\varepsilon(v', w') = \sigma_0(\iota(v'), \iota(w'))$ via a case analysis.

First, suppose that $\sigma_0(\iota(v'), \iota(w')) = 1$: here, we need to show that v' and w' are consistent. The respective formulas $\phi(\iota(v'))$ and $\phi(\iota(w'))$ only share common variables in clauses of the form $(q_j \Rightarrow p(v'))$ and $(q_j \Rightarrow p(w'))$. These formulas and their natural language expressions are both consistent unless $p(v') = \neg p(w')$, which can only occur if $\sigma_0(\iota(v'), \iota(w')) = -1$, a contradiction.

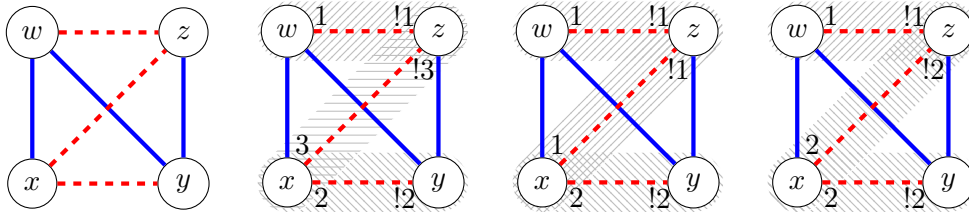


Figure 5: Left: a clique in a notional signed coherence graph. Center left: the degenerate star forest decomposition of negative edges yields the greatest number of corresponding properties. The notations n and $!n$ respectively indicate inconsistent propositional clauses of the form $(q \Rightarrow p_n)$ and $(q \Rightarrow \neg p_n)$. For example, if $\Rightarrow p_1$, $\Rightarrow p_2$, and $\Rightarrow p_3$ respectively correspond to “is hot,” “is bright,” and “is loud,” then a natural language expression of modeling propositions is $\{w' : (q \text{ is hot}), x' : (q \text{ is bright AND loud}), y' : (q \text{ is dark}), z' : (q \text{ is cold AND quiet})\}$. Right panels: the two star forest decompositions of minimal size yield the minimal number of corresponding properties. The panel on the right corresponds to $\{w' : (q \text{ is hot}), x' : (q \text{ is bright}), y' : (q \text{ is dark}), z' : (q \text{ is cold AND dark})\}$.

Next, suppose that $\sigma_0(\iota(v'), \iota(w')) = 0$: here, we need to show that v' and w' are independent. Now $\iota(v')$ and $\iota(w')$ are not in a common clique, so the respective formulas $\phi(\iota(v'))$ and $\phi(\iota(w'))$ do not share any common variables. The required result follows.

Finally, suppose that $\sigma_0(\iota(v'), \iota(w')) = -1$: here, we need to show that v' and w' are inconsistent. Now the formulas $\phi(\iota(v'))$ and $\phi(\iota(w'))$ respectively contain clauses of the form $(q_j \Rightarrow p_k)$ and $(q_j \Rightarrow \neg p_k)$ for some clique C_j and star forest F_k in the graph induced by E_j^- . Thus both the formulas and their natural language expressions are inconsistent. ■

Note that Algorithm 1 does not require a specific construction for clique edge covers or for star forest decompositions. Different constructions affect the numbers of variables and properties: see §E for different clique edge cover approaches. While the approach of Conte et al. (2020) gives practical linear-time performance for clique edge covers on graphs of thousands to millions of vertices, we deal with smaller graphs and we can therefore employ more pedestrian techniques:

- *degenerate*: take the degenerate clique edge cover formed by individual edges;
- *percolation*: find all maximal cliques, then use a constraint solver to optimize a clique edge cover (see <https://stackoverflow.com/a/49145938>);
- *partition*: initialize $G' = G$, then greedily partition $E(G')$ by iteratively removing edges from the largest clique, as discussed in but avoided by Conte et al. (2020).

Note that the first and last of these techniques actually yield a clique edge partition.

Practical algorithms are in shorter supply for star forest decompositions. Finding small decompositions is NP-complete (Hakimi et al., 1996). An integer linear program for star decompositions (to be aggregated into star forest decompositions) is described in Hajebi and Javadi (2024), while Cicalese and Laber (2021) gives a linear time (1/2)-approximation algorithm for the largest minimum star size. An arboricity-realizing algorithm such as Gabow and Westermann (1988) yields a (1/2)-approximate star arboricity-realizing algorithm by the observation of Alon et al. (1992) that any tree can be covered by two star forests. Here we only use the second of the following techniques:

Algorithm 1 MODELCOHERENCEGRAPH(G_σ)

Require: Signed coherence graph G_σ

```

1: Produce a clique edge cover  $C = \{C_1, \dots, C_m\}$  of  $G_\sigma$ 
2: for  $v \in V = V(G_\sigma)$  do
3:    $\phi(v) \leftarrow \emptyset$  // initialize with empty propositional formula
4: for  $C_j \in C$  do
5:    $E_j^- \leftarrow \{(v, w) \in E(C_j) : \sigma(v, w) = -1\}$ 
6:   Produce a star forest decomposition  $F = \{F_1, \dots, F_n\}$  of the graph induced by  $E_j^-$ 
7:   for  $F_k \in F$  do
8:     for each star  $S \subseteq F_k$  do
9:        $r \leftarrow$  root of  $S$ 
10:       $\phi(r) \leftarrow \phi(r) \wedge (q_j \Rightarrow p_k)$  // "...AND  $q_j$  has property  $p_k$ "
11:      for each leaf vertex  $\ell \in S$  do
12:         $\phi(\ell) \leftarrow \phi(\ell) \wedge (q_j \Rightarrow \neg p_k)$  // "...AND  $q_j$  has property NOT( $p_k$ )"
13: for  $v \in V$  do
14:   if  $\phi(v) = \emptyset$  then
15:      $\phi(v) \leftarrow (q_v^* \Rightarrow p_v^*)$  // to avoid triviality;  $q_v^*$  only appears in  $\phi(v)$ 
16:      $v' \leftarrow$  natural language expression of  $\phi(v)$  // see comments above
17:      $\iota(v') \leftarrow v$ 

```

Ensure: $\{\iota^{-1}(v) : v \in V\} = V' \models G_\sigma$

- take the degenerate star forest decomposition formed by individual edges;
- use the (1/2)-approximate algorithm for the largest minimum star size;
- repeatedly generate uniformly random edge partitions (Stam, 1983) and test that they contain no triangles or simple paths of (edge) length 3 (Aider et al., 2019): this is a viable brute force strategy for connected components on up to about 10 vertices since the corresponding number of partitions—i.e., the Bell number B_{10} —is 115975.

2.2. Benchmarking coherence

Because computing coherence amounts to solving MAX-CUT (or MAX-SAT more generally as in §A.2), benchmarking CDI is mainly a question of fidelity of coherence graph reconstruction. Runtime and approximation performance of combinatorial optimization algorithms in §A may become important, but at scales considered here, exact solutions are always computationally feasible.⁴

The propositions we generate for benchmarking use a grammar that can represent multiple types of relations and uncertainty (see §D.1). We note that the specific syntax used to represent propositions in the benchmark dataset is a matter of convenience, and the benchmark can be adapted to represent synthetic propositions using any syntax that is suitable for a given application.

4. Inferring a coherence graph from a set of propositions is similar to classical natural language inference or textual entailment (Korman et al., 2018), which involves evaluating the logical relationship between two sentences (see §F). However, explanatory coherence describes more general properties of individual propositions and sets of propositions in the context of theory formation. Further, coherence encompasses a range of relations that include deductive entailment but also explanatory, analogical, perceptual, conceptual, and deliberative relations (Thagard, 2002).

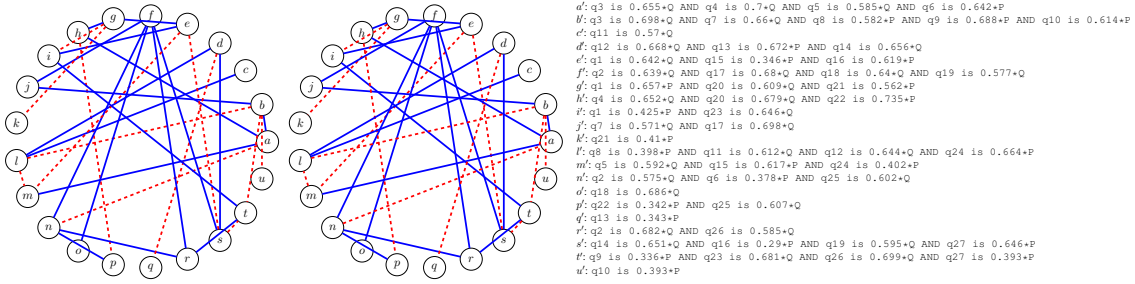


Figure 6: Left: a coherence graph from our benchmark with edge density target 0.15 (“sparse”). Center: o1-mini achieved perfect reconstruction on this example under high uncertainty. Right: the modeling propositions incorporated high uncertainty (see §D).

We use a “micro” F_1 score to evaluate fidelity of coherence graph reconstruction for each attempt. This accounts for class imbalance among the values in $\{-1, 0, 1\}$ for each entry in each synthetic adjacency matrix included in our evaluation task (Opitz, 2024).⁵

3. Experimental setup

We include models intentionally designed for reasoning in our evaluation. We refer to o1/3/4-mini (Jaech et al., 2024; OpenAI, 2025), QwQ-32B (Qwen, 2024), and Sky-T1-32B (NovaSky, 2025) as *large reasoning models* (LRMs), following the phrasing of Valmeekam et al. (2024) to describe models designed to generate long chains of thought at inference time. These models have high latency and inference costs (Abdin et al., 2024). We call phi-4 (Abdin et al., 2024) a *small language model* (SLM). We call the remaining models LLMs: gemini-2.0-flash-exp (DeepMind, 2024), claude-3.5-sonnet (Anthropic, 2024), gpt-4o (Hurst et al., 2024), llama-3.3-70B (Meta, 2024), llama-4-scout (Meta, 2025), and gemini-1.5-pro (Pichai and Hassabis, 2024). For all models, we post-processed outputs to extract structured data for evaluation.

NB. We are still benchmarking a DeepSeek model as of this writing. We further plan to evaluate other models (e.g., GPT-5, more recent versions of Gemini and Sonnet and other Llama versions/derivatives), and to report results in an update.

3.1. Benchmark generation

To instantiate our benchmark, we sample signed coherence graphs from an Erdős-Rényi (ER) distribution. We ensure that each sample graph is fully connected by joining sampled graphs to a minimum spanning tree generated for a complete graph of equivalent size with random edge weights.

For comparison with practical examples, the degree variance goodness-of-fit test in Ouadah et al. (2020) and Brune et al. (2025) fails to reject the ER hypothesis for the (unweighted version of the) graph in Figure 2. However, the same test does reject the ER hypothesis for graphs in Figure 3 with p -values around 0.001. Other realistic examples not detailed here also fall into both categories.

We generate 76 graphs with $5 \leq |V| \leq 23$, targeting two regimes of edge density $:= |E|/\binom{|V|}{2}$: sparse has a median edge density of 0.202 and dense has a median edge density of 0.734.

5. Another approach to gauging performance is to use a distance measure, as in §K.

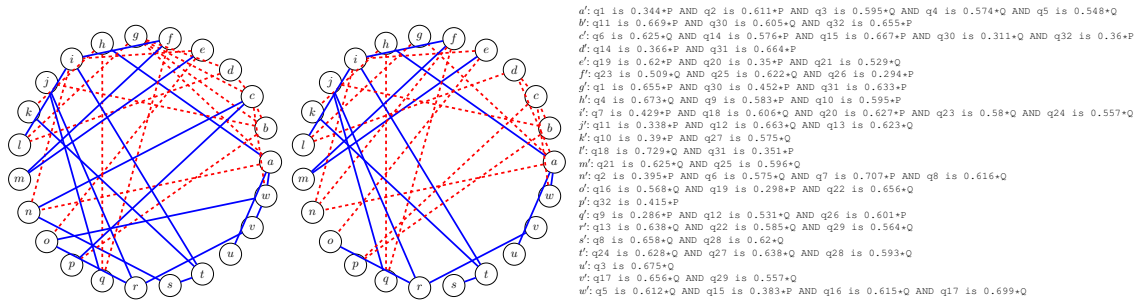


Figure 7: Left: another coherence graph from our benchmark with edge density target 0.15 (“sparse”). Center: o1-mini achieved good but imperfect ($F_1 = 0.96$: see vertices $c, d, g, n,$ and o) reconstruction on this example under high uncertainty. Right: the modeling propositions incorporated high uncertainty (see §D).

This yields proposition sets involving variable and property counts as detailed in §G. For each problem, we generate four additional sets of propositions. Three of these correspond to the noise regimes described in §D.1. We also generate a set of propositions where we add no noise (i.e., $p \leftarrow 1 * p$ and $\neg p \leftarrow 0 * P$) in order to control for the presence of distractors in the evaluation.

Figure 6 shows a problem from the benchmark including a synthetic coherence graph with 21 vertices, modeling propositions, and o1-mini’s perfect graph reconstruction (which occurs half the time, as Figure 8 shows). Figure 7 is similar, but with imperfect reconstruction.

3.2. Prompts

We use a common prompt structure shown in §I that a) establishes the consistency reasoning task, b) describes variables and properties relevant for evaluating a set of propositions, c) sets fuzzy membership thresholds for properties (see §D.1) and d) embeds propositions for a given problem.

4. Results

4.1. LLMs successfully infer synthetic coherence graphs from a single prompt

Model performance varies considerably, with o1/3/4-mini, claude-3.5-sonnet and QwQ-32B outperforming the other models for both sparse and dense problems: see Figure 8.

4.2. Minor post-processing is sometimes necessary to handle obvious reconstruction errors

We noted four general types of reconstruction errors. First, some reconstructed graphs do not include a given proposition seen in the prompt. We observed this sporadically in all models. Second, we noticed some instances with Gemini models where the reconstructed graph contains nodes named, for instance, ”Proposition(a)” instead of a or ”(a)” instead of a. We noticed instances where QwQ incorrectly capitalized proposition names, for instance, substituting ”A” for ”a”. We correct these first three error types in post-processing before evaluation.

Finally, we observed that some models hallucinate extra propositions in the reconstructed graph. Out of 608 inference attempts, gemini-2.0-flash-exp hallucinates on 10 inference attempts,

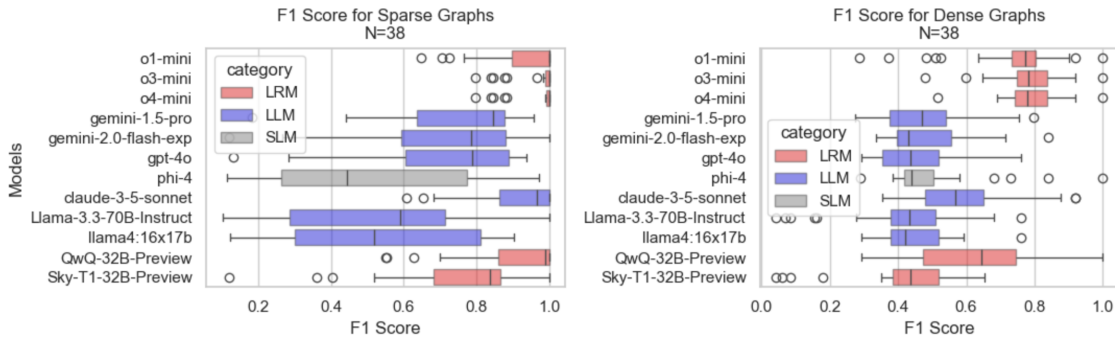


Figure 8: o1/3/4-mini, claude-3.5-sonnet, and QwQ-32B have high micro F_1 scores.

gpt-4o on 5, gemini-1.5-pro on 4, and Sky-T1-32B on 1. We do not correct this type of error with post-processing; we instead eliminate these inference attempts from evaluation for these models since these hallucinations can be easily detected at runtime.

5. Conclusion

While our main result is a demonstration that some LLMs can reconstruct signed coherence graphs with high fidelity, an ideal is to connect a benchmark with realistic examples.⁶ This involves two factors: topology and weights. Regarding topology, some realistic examples we have examined are compatible with the ER hypothesis, and others are not. However, our basic approach is compatible with any signed graph topology model (including empirical results from coherence graph construction itself). It is important to note also that in the present context, topology also refers to the structure of cliques and star forest decompositions, both of which admit significant variation to be considered in future work along with underlying graph characteristics beyond uniform sparsity. Regarding weights, extensions of our benchmark to incorporate weights in $[-1, 1]$ by (e.g.) building on §D and a weighted stochastic block model (Aicher et al., 2015) are left for future work.

Other future extensions of the work could include benchmarking more recent models and variants; deeper analyses along the lines of our appendices, and alternative prompting strategies (e.g., block-decomposing the space of proposition pairs) that are relevant for scaling.

CDI provides a good model for many forms of cognition, including perception and planning. Combining CDI with consistency evaluations by neural models may lead to advancements in the state of the art in these tasks. Moreover, our results indicate that it is now feasible to computationally instantiate a coherence theory of truth (Young, 2024). By hard-coding conclusively established propositions, this theory can be anchored in a correspondence theory of truth (David, 2022).

References

Marah Abdin, Jyoti Aneja, Harkirat Behl, Sébastien Bubeck, Ronen Eldan, Suriya Gunasekar, Michael Harrison, Russell J Hewett, Mojan Javaheripi, Piero Kauffmann, et al. Phi-4 technical

6. It appears that o3/4-mini significantly outperform o1-mini in practice on more complex (not larger *per se*) real-world instances. However, our results are still too preliminary to be appropriate to detail here.

- report. *arXiv preprint arXiv:2412.08905*, 2024. URL <https://arxiv.org/abs/2412.08905>.
- Christopher Aicher, Abigail Z Jacobs, and Aaron Clauset. Learning latent block structure in weighted networks. *Journal of Complex Networks*, 3(2):221–248, 2015. URL <https://doi.org/10.1093/comnet/cnu026>.
- Méziane Aïder, Lamia Aoudia, Mourad Baiou, A Ridha Mahjoub, and Viet Hung Nguyen. On the star forest polytope for trees and cycles. *RAIRO-Operations Research*, 53(5):1763–1773, 2019. URL <https://doi.org/10.1051/ro/2018076>.
- Jin Akiyama and Mikio Kano. Factors and factorizations of graphs—a survey. *Journal of Graph Theory*, 9(1):1–42, 1985. URL <https://doi.org/10.1002/jgt.3190090103>.
- Noga Alon, Colin McDiarmid, and Bruce Reed. Star arboricity. *Combinatorica*, 12:375–380, 1992. URL <https://doi.org/10.1007/BF01305230>.
- Anthropic. Claude 3.5 Sonnet: raising the bar for intelligence. <https://www.anthropic.com/news/claude-3-5-sonnet>, 2024. Accessed: January 2025.
- András A Benczúr and David R Karger. Approximating s - t minimum cuts in $\tilde{O}(n^2)$ time. In *Symposium on Theory of Computing*, pages 47–55, 1996. URL <https://doi.org/10.1145/237814.237827>.
- Yoshua Bengio and Nikolay Malkin. Machine learning and information theory concepts towards an AI mathematician. *Bulletin of the American Mathematical Society*, 61(3):457–469, 2024. URL <https://doi.org/10.1090/bull/1839>.
- Mark Blokpoel and Iris van Rooij. *Theoretical Modeling for Cognitive Science and Psychology*. 2024. URL <https://computationalcognitivescience.github.io/lovelace/home>.
- Tom Brown, Benjamin Mann, Nick Ryder, Melanie Subbiah, Jared D Kaplan, Prafulla Dhariwal, Arvind Neelakantan, Pranav Shyam, Girish Sastry, Amanda Askell, et al. Language models are few-shot learners. *Advances in Neural Information Processing Systems*, 33:1877–1901, 2020. URL <https://arxiv.org/abs/2005.14165>.
- Barbara Brune, Jonathan Flossdorf, and Carsten Jentsch. Goodness-of-fit testing based on graph functionals for homogeneous Erdős–Rényi graphs. *Scandinavian Journal of Statistics*, 52(1):332–380, 2025. URL <https://doi.org/10.1111/sjos.12750>.
- Norishige Chiba and Takao Nishizeki. Arboricity and subgraph listing algorithms. *SIAM Journal on Computing*, 14(1):210–223, 1985. URL <https://doi.org/10.1137/0214017>.
- Ferdinando Cicalese and Eduardo Sany Laber. On the star decomposition of a graph: hardness results and approximation for the max–min optimization problem. *Discrete Applied Mathematics*, 289:503–515, 2021. URL <https://doi.org/10.1016/j.dam.2020.07.014>.
- Alessio Conte, Roberto Grossi, and Andrea Marino. Large-scale clique cover of real-world networks. *Information and Computation*, 270:104464, 2020. URL <https://doi.org/10.1016/j.ic.2019.104464>.

- Natalia Criado, Elizabeth Black, and Michael Luck. A coherence maximisation process for solving normative inconsistencies. *Autonomous Agents and Multi-Agent Systems*, 30:640–680, 2016. URL <https://doi.org/10.1007/s10458-015-9300-x>.
- Marian David. The correspondence theory of truth. In Edward N. Zalta, editor, *The Stanford Encyclopedia of Philosophy*. Metaphysics Research Lab, Stanford University, Summer 2022 edition, 2022. <https://plato.stanford.edu/archives/sum2022/entries/truth-correspondence/>.
- DeepMind. Gemini 2.0 Flash Experimental. <https://deepmind.google/technologies/gemini/flash/>, 2024. Accessed: January 2025.
- DNI. Intelligence community directive 203: Analytic standards. <https://irp.fas.org/dni/icd/icd-203.pdf>, January 2 2015. Director of National Intelligence.
- Paul Erdős, Adolph W Goodman, and Louis Pósa. The representation of a graph by set intersections. *Canadian Journal of Mathematics*, 18:106–112, 1966. URL <https://doi.org/10.4153%2FCJM-1966-014-3>.
- Jiazhan Feng, Ruochen Xu, Junheng Hao, Hiteshi Sharma, Yelong Shen, Dongyan Zhao, and Weizhu Chen. Language models can be deductive solvers. In *Findings of the Association for Computational Linguistics*, pages 4026–4042, 2024. URL <https://doi.org/10.18653/v1/2024.findings-naacl.254>.
- Scott Ferson, Jason O’Rawe, Andrei Antonenko, Jack Siegrist, James Mickley, Christian C Luhmann, Kari Sentz, and Adam M Finkel. Natural language of uncertainty: numeric hedge words. *International Journal of Approximate Reasoning*, 57:19–39, 2015. URL <https://doi.org/10.1016/j.ijar.2014.11.003>.
- William M Fogarty. Formal investigation into the circumstances surrounding the downing of Iran Air flight 655 on 3 July 1988. Technical report, US Department of Defense, 1988. URL <https://apps.dtic.mil/sti/citations/ADA203577>. See also https://en.wikisource.org/wiki/Formal_Investigation_into_the_Circumstances_Surrounding_the_Downing_of_Iran_Air_Flight_655_on_3_July_1988/Formal_Report.
- M Laura Frigotto and Alessandro Rossi. An explanatory coherence model of decision making in ill-structured problems. *Mind & Society*, 14:35–55, 2015. URL <https://doi.org/10.1007/s11299-014-0158-4>.
- Harold Gabow and Herbert Westermann. Forests, frames, and games: algorithms for matroid sums and applications. In *Symposium on Theory of Computing*, pages 407–421, 1988. URL <https://doi.org/10.1145/62212.62252>.
- Bernd Gärtner and Jiri Matousek. *Approximation Algorithms and Semidefinite Programming*. Springer, 2012. URL <https://doi.org/10.1007/978-3-642-22015-9>.
- Jonathan L Gross, Jay Yellen, and Mark Anderson. *Graph Theory and its Applications*. CRC, 2018. URL <https://doi.org/10.1201/9780429425134>.

- Sahab Hajebi and Ramin Javadi. Parameterized complexity of star decomposition problem. *arXiv preprint arXiv:2411.13348*, 2024. URL <https://arxiv.org/abs/2411.13348>.
- S Louis Hakimi, John Mitchem, and Edward Schmeichel. Star arboricity of graphs. *Discrete Mathematics*, 149(1-3):93–98, 1996. URL [https://doi.org/10.1016/0012-365X\(94\)00313-8](https://doi.org/10.1016/0012-365X(94)00313-8).
- Simeng Han, Hailey Schoelkopf, Yilun Zhao, Zhenting Qi, Martin Riddell, Wenfei Zhou, James Coady, David Peng, Yujie Qiao, Luke Benson, et al. FOLIO: natural language reasoning with first-order logic. *arXiv preprint arXiv:2209.00840*, 2022. URL <https://arxiv.org/abs/2209.00840>.
- Keith J Holyoak and Dan Simon. Bidirectional reasoning in decision making by constraint satisfaction. *Journal of Experimental Psychology: General*, 128(1):3, 1999. URL <https://psycnet.apa.org/doi/10.1037/0096-3445.128.1.3>.
- Steve Huntsman, August 2024. URL <https://github.com/SteveHuntsman/LegalCoherence/tree/main/Vincennes>. Accessed: February 2025.
- Steve Huntsman, Michael Robinson, and Ludmilla Huntsman. Prospects for inconsistency detection using large language models and sheaves. *arXiv preprint arXiv:2401.16713*, 2024. URL <https://arxiv.org/abs/2401.16713>.
- Aaron Hurst, Adam Lerer, Adam P Goucher, Adam Perelman, Aditya Ramesh, Aidan Clark, AJ Ostrow, Akila Welihinda, Alan Hayes, Alec Radford, et al. GPT-4o system card. *arXiv preprint arXiv:2410.21276*, 2024. URL <https://arxiv.org/abs/2410.21276>.
- Aaron Jaech, Adam Kalai, Adam Lerer, Adam Richardson, Ahmed El-Kishky, Aiden Low, Alec Helyar, Aleksander Madry, Alex Beutel, Alex Carney, et al. OpenAI o1 system card. *arXiv preprint arXiv:2412.16720*, 2024. URL <https://arxiv.org/abs/2412.16720>.
- Stephen P Jordan, Noah Shutty, Mary Wootters, Adam Zalcman, Alexander Schmidhuber, Robbie King, Sergei V Isakov, and Ryan Babbush. Optimization by decoded quantum interferometry. *arXiv preprint arXiv:2408.08292*, 2024. URL <https://arxiv.org/abs/2408.08292>.
- Sindhu Joseph and Henry Prakken. Coherence-driven argumentation to norm consensus. In *International Conference on Artificial Intelligence and Law*, pages 58–67, 2009. URL <https://doi.org/10.1145/1568234.1568242>.
- Anatoly Kachynskiy. National security assessment method based on fuzzy sets theory. *Theoretical and Applied Cybersecurity*, 1(1), 2019. URL <https://doi.org/10.20535/tacs.2664-29132019.1.169084>.
- Daniel Kahneman. *Thinking, Fast and Slow*. Farrar, Straus and Giroux, 2011.
- Vedant Khandelwal, Vishal Pallagani, Biplav Srivastava, and Francesca Rossi. A neurosymbolic fast and slow architecture for graph coloring. *arXiv preprint arXiv:2412.01752*, 2024. URL <https://arxiv.org/abs/2412.01752>.

- Subhash Khot, Guy Kindler, Elchanan Mossel, and Ryan O’Donnell. Optimal inapproximability results for MAX-CUT and other 2-variable CSPs? *SIAM Journal on Computing*, 37(1):319–357, 2007. URL <https://doi.org/10.1137/S0097539705447372>.
- Daniel Z Korman, Eric Mack, Jacob Jett, and Allen H Renear. Defining textual entailment. *Journal of the Association for Information Science and Technology*, 69(6):763–772, 2018. URL <https://doi.org/10.1002/asi.24007>.
- Jomon Kottarathil, Sudev Naduvath, and Joseph Varghese Kureethara. *Graph Theory and Decomposition*. CRC, 2024. URL <https://doi.org/10.1201/9781003391678>.
- Michael Krisper, Jürgen Dobaj, and Georg Macher. Patterns for communicating numerical uncertainty. In *European Conference on Pattern Languages of Programs*, pages 1–15, 2019. URL <https://doi.org/10.1145/3361149.3361160>.
- Bimal Kumar and Dmitri Roussinov. NLP-based regulatory compliance—using GPT 4.0 to decode regulatory documents. *arXiv preprint arXiv:2412.20602*, 2024. URL <https://arxiv.org/abs/2412.20602>.
- Arthur Lee and Bruce Xu. Classifying approximation algorithms: understanding the APX complexity class. *arXiv preprint arXiv:2111.01551*, 2021. URL <https://arxiv.org/abs/2111.01551>.
- Doug Lenat and Gary Marcus. Getting from generative AI to trustworthy AI: What LLMs might learn from Cyc. *arXiv preprint arXiv:2308.04445*, 2023. URL <https://arxiv.org/abs/2308.04445>.
- Chu Min Li, Felip Manyà, Joan Ramon Soler, and Amanda Vidal. Clausal forms in MaxSAT and MinSAT. *International Journal of Computational Intelligence Systems*, 15(1):97, 2022. URL <https://doi.org/10.1007/s44196-022-00143-z>.
- Jiacheng Liu, Sewon Min, Luke Zettlemoyer, Yejin Choi, and Hannaneh Hajishirzi. Infinigram: scaling unbounded n -gram language models to a trillion tokens. *arXiv preprint arXiv:2401.17377*, 2024. URL <https://arxiv.org/abs/2401.17377>.
- Maximilian Maier, Noah van Dongen, and Denny Borsboom. Comparing theories with the Ising model of explanatory coherence. *Psychological Methods*, 2023. URL <https://doi.org/10.1037/met0000543>.
- Giuseppe Marra, Sebastijan Dumančić, Robin Manhaeve, and Luc De Raedt. From statistical relational to neurosymbolic artificial intelligence: a survey. *Artificial Intelligence*, page 104062, 2024. URL <https://doi.org/10.1016/j.artint.2023.104062>.
- William Merrill and Ashish Sabharwal. The expressive power of transformers with chain of thought. In *International Conference on Learning Representations*, 2024. URL <https://arxiv.org/abs/2310.07923>.
- Meta. The Meta Llama 3.3 multilingual large language model (LLM). https://github.com/meta-llama/llama-models/blob/main/models/llama3_3/MODEL_CARD.md, 2024. Accessed: January 2025.

- Meta. The Llama 4 collection of models. https://github.com/meta-llama/llama-models/blob/main/models/llama4/MODEL_CARD.md, 2025. Accessed: May 2025.
- Marc Mezard and Andrea Montanari. *Information, Physics, and Computation*. Oxford, 2009. URL <https://doi.org/10.1093/acprof:oso/9780198570837.001.0001>.
- Cristopher Moore and Stephan Mertens. *The Nature of Computation*. Oxford, 2011. URL <https://doi.org/10.1093/acprof:oso/9780199233212.001.0001>.
- Neel Nanda, Lawrence Chan, Tom Lieberum, Jess Smith, and Jacob Steinhardt. Progress measures for grokking via mechanistic interpretability. In *International Conference on Learning Representations*, 2023. URL <https://openreview.net/forum?id=9XF5bDPmdW>.
- Balas Kausik Natarajan. Sparse approximate solutions to linear systems. *SIAM Journal on Computing*, 24(2):227–234, 1995. URL <https://doi.org/10.1137/S0097539792240406>.
- NovaSky. Sky-T1: fully open-source reasoning model with o1-preview performance in \$450 budget, 2025. URL <https://novasky-ai.github.io/posts/sky-t1>. Accessed: January 2025.
- Franz Nowak, Anej Svete, Alexandra Butoi, and Ryan Cotterell. On the representational capacity of neural language models with chain-of-thought reasoning. *arXiv preprint arXiv:2406.14197*, 2024. URL <https://arxiv.org/abs/2406.14197>.
- Theo Olausson, Alex Gu, Ben Lipkin, Cedegao Zhang, Armando Solar-Lezama, Joshua Tenenbaum, and Roger Levy. LINC: a neurosymbolic approach for logical reasoning by combining language models with first-order logic provers. In *Empirical Methods in Natural Language Processing*, pages 5153–5176, 2023. URL <https://doi.org/10.18653/v1/2023.emnlp-main.313>.
- OpenAI. OpenAI o3 and o4-mini system card. <https://openai.com/index/o3-o4-mini-system-card/>, 2025. Accessed: May 2025.
- Juri Opitz. A closer look at classification evaluation metrics and a critical reflection of common evaluation practice. *Transactions of the Association for Computational Linguistics*, 12:820–836, 2024. URL https://doi.org/10.1162/tacl_a_00675.
- Sarah Ouadah, Stéphane Robin, and Pierre Latouche. Degree-based goodness-of-fit tests for heterogeneous random graph models: independent and exchangeable cases. *Scandinavian Journal of Statistics*, 47(1):156–181, 2020. URL <https://doi.org/10.1111/sjos.12410>.
- Liangming Pan, Alon Albalak, Xinyi Wang, and William Wang. Logic-LM: empowering large language models with symbolic solvers for faithful logical reasoning. In *Empirical Methods in Natural Language Processing*, pages 3806–3824, 2023. URL <https://doi.org/10.18653/v1/2023.findings-emnlp.248>.
- Binghui Peng, Srinu Narayanan, and Christos Papadimitriou. On limitations of the transformer architecture. In *Conference on Language Models*, 2024. URL <https://arxiv.org/abs/2402.08164>.

- Jorge Pérez, Pablo Barceló, and Javier Marinkovic. Attention is Turing-complete. *Journal of Machine Learning Research*, 22(75):1–35, 2021. URL <https://www.jmlr.org/papers/v22/20-302.html>.
- Sundar Pichai and Demis Hassabis. Our next-generation model: Gemini 1.5, February 2024. URL <https://blog.google/technology/ai/google-gemini-next-generation-model-february-2024/>. Accessed: January 2025.
- Qwen. QwQ: reflect deeply on the boundaries of the unknown, November 2024. URL <https://qwenlm.github.io/blog/qwq-32b-preview/>. Accessed: February 2025.
- Charles C Ragin. Set relations in social research: evaluating their consistency and coverage. *Political Analysis*, 14(3):291–310, 2006. URL <https://doi.org/10.1093/pan/mpj019>.
- Nived Rajaraman, Marco Bondaschi, Ashok Vardhan Makkuva, Kannan Ramchandran, and Michael Gastpar. Transformers on Markov data: constant depth suffices. In *Neural Information Processing Systems*, 2024. URL <https://arxiv.org/abs/2407.17686>.
- Nils Reimers and Iryna Gurevych. Sentence-BERT: sentence embeddings using Siamese BERT-networks, 2019. URL <https://arxiv.org/abs/1908.10084>.
- H. A. Ripley. *Minute Mysteries*. Houghton Mifflin, 1932. URL https://www.gutenberg.org/files/50603/50603-h/50603-h.htm#mys_1.
- Daniel Rosiak. *Sheaf Theory Through Examples*. MIT, 2022. URL <https://doi.org/10.7551/mitpress/12581.001.0001>.
- Amitabha Roy. Fault tolerant Boolean satisfiability. *Journal of Artificial Intelligence Research*, 25: 503–527, 2006. URL <https://doi.org/10.1613/jair.1914>.
- Abulhair Saparov and He He. Language models are greedy reasoners: a systematic formal analysis of chain-of-thought. In *International Conference on Learning Representations*, 2023. URL <https://arxiv.org/abs/2210.01240>.
- Md Kamruzzaman Sarker, Lu Zhou, Aaron Eberhart, and Pascal Hitzler. Neuro-symbolic artificial intelligence: current trends. *AI Communications*, 34(3):197–209, 2022. URL <https://doi.org/10.3233/AIC-210084>.
- Lesia Semenova, Cynthia Rudin, and Ronald Parr. On the existence of simpler machine learning models. In *Conference on Fairness, Accountability, and Transparency*, pages 1827–1858, 2022. URL <https://doi.org/10.1145/3531146.3533232>.
- Damien Sileo. Tasksource: a large collection of NLP tasks with a structured dataset preprocessing framework. In *Joint International Conference on Computational Linguistics, Language Resources and Evaluation (LREC-COLING)*, pages 15655–15684, Torino, Italia, May 2024. ELRA and ICCL. URL <https://aclanthology.org/2024.lrec-main.1361>.
- Dan Simon. A third view of the black box: cognitive coherence in legal decision making. *University of Chicago Law Review*, 71(2):511, 2004. URL <https://chicagounbound.uchicago.edu/uclrev/vol71/iss2/3/>.

- Sunit Sivaraj and Levent Yilmaz. Cogent: a coherence-driven cognitive agent modelling and experimentation framework. *International Journal of Simulation and Process Modelling*, 14(1):36–50, 2019. URL <https://doi.org/10.1504/IJSPM.2019.097707>.
- Tasuku Soma and Yuichi Yoshida. Spectral sparsification of hypergraphs. In *Symposium on Discrete Algorithms*, pages 2570–2581. SIAM, 2019. URL <https://doi.org/10.1137/1.9781611975482.159>.
- Daniel A Spielman and Shang-Hua Teng. Spectral sparsification of graphs. *SIAM Journal on Computing*, 40(4):981–1025, 2011. URL <https://doi.org/10.1137/08074489X>.
- Yellamraju V Srinivas. Applications of sheaf theory in algorithm design. Technical report, Kestrel Institute, 1993. URL <https://apps.dtic.mil/sti/citations/ADA272724>.
- AJ Stam. Generation of a random partition of a finite set by an urn model. *Journal of Combinatorial Theory, Series A*, 35(2):231–240, 1983. URL [https://doi.org/10.1016/0097-3165\(83\)90009-2](https://doi.org/10.1016/0097-3165(83)90009-2).
- Paul Thagard. Adversarial problem solving: modeling an opponent using explanatory coherence. *Cognitive Science*, 16(1):123–149, 1992. URL [https://doi.org/10.1016/0364-0213\(92\)90019-Q](https://doi.org/10.1016/0364-0213(92)90019-Q).
- Paul Thagard. *Coherence in Thought and Action*. MIT, 2002. URL <https://doi.org/10.7551/mitpress/1900.001.0001>.
- Paul Thagard. Causal inference in legal decision making: explanatory coherence vs. Bayesian networks. *Applied Artificial Intelligence*, 18(3-4):231–249, 2004. URL <https://doi.org/10.1080/08839510490279861>.
- Paul Thagard and Karsten Verbeurgt. Coherence as constraint satisfaction. *Cognitive Science*, 22(1):1–24, 1998. URL [https://doi.org/10.1016/S0364-0213\(99\)80033-0](https://doi.org/10.1016/S0364-0213(99)80033-0).
- Thucydides. *History of the Peloponnesian War*. Longmans, Green, and Co., 1874. URL <https://www.gutenberg.org/files/7142/7142-h/7142-h.htm#link2HCH0017>.
- Karthik Valmееkam, Kaya Stechly, and Subbarao Kambhampati. LLMs still can’t plan; can LRMs? A preliminary evaluation of OpenAI’s o1 on PlanBench. *arXiv preprint arXiv:2409.13373*, 2024. URL <https://arxiv.org/abs/2409.13373>.
- Iris Van Rooij. The tractable cognition thesis. *Cognitive science*, 32(6):939–984, 2008. URL <https://doi.org/10.1080/03640210801897856>.
- Iris Van Rooij, Mark Blokpoel, Johan Kwisthout, and Todd Wareham. *Cognition and Intractability: A Guide to Classical and Parameterized Complexity Analysis*. Cambridge, 2019. URL <https://doi.org/10.1017/9781107358331>.
- Ashish Vaswani, Noam Shazeer, Niki Parmar, Jakob Uszkoreit, Llion Jones, Aidan N Gomez, Łukasz Kaiser, and Illia Polosukhin. Attention is all you need. *Advances in Neural Information Processing Systems*, 30:5998–6008, 2017. URL <https://arxiv.org/abs/1706.03762>.

- Vijay V Vazirani. *Approximation Algorithms*. Springer, 2001. URL <https://doi.org/10.1007/978-3-662-04565-7>.
- Martin J Wainwright, Elitza Maneva, and Emin Martinian. Lossy source compression using low-density generator matrix codes: analysis and algorithms. *IEEE Transactions on Information Theory*, 56(3):1351–1368, 2010. URL <https://doi.org/10.1109/TIT.2009.2039160>.
- Xi Ye, Qiaochu Chen, Isil Dillig, and Greg Durrett. SatLM: satisfiability-aided language models using declarative prompting. *Advances in Neural Information Processing Systems*, 36, 2024. URL <https://arxiv.org/abs/2305.09656>.
- Levent Yilmaz, Ana Franco-Watkins, and Timothy S Kroecker. Computational models of ethical decision-making: a coherence-driven reflective equilibrium model. *Cognitive Systems Research*, 46:61–74, 2017. URL <https://doi.org/10.1016/j.cogsys.2017.02.005>.
- James O Young. The coherence theory of truth. In Edward N. Zalta and Uri Nodelman, editors, *The Stanford Encyclopedia of Philosophy*. Metaphysics Research Lab, Stanford University, Summer 2024 edition, 2024. <https://plato.stanford.edu/archives/sum2024/entries/truth-coherence/>.
- Wanjun Zhong, Siyuan Wang, Duyu Tang, Zenan Xu, Daya Guo, Jiahai Wang, Jian Yin, Ming Zhou, and Nan Duan. AR-LSAT: investigating analytical reasoning of text. *arXiv preprint arXiv:2104.06598*, 2021. URL <https://arxiv.org/abs/2104.06598>.

Appendix A. Coherence can be computed in different ways

A.1. Classical coherence is equivalent to 2-MAX-XORSAT and to sparse approximation for 2-XORSAT

There are a number of algorithms for computing coherence classically. Besides a brute force solution to the MAX-CUT problem for a coherence graph G_σ , there are also greedy stochastic, simulated annealing, and semidefinite programming approximations (Thagard and Verbeurgt, 1998; Gärtner and Matousek, 2012). Historically, the dominant approach is a dynamical neural (“connectionist”) algorithm discussed in Thagard (2002). However, implementations are sufficiently outdated or hard to work with⁷ that an adaptation based on an Ising model has recently been developed (Maier et al., 2023).

We proceed to outline two computational perspectives on coherence that to our knowledge have not previously been considered explicitly, though the second was discussed at the level of prose in Huntsman et al. (2024). Given a coherence graph G_σ , the consistency equation $\sigma(v, w) = 1$ corresponds to an equation of the form $x_v + x_w = 0$ over the Boolean field \mathbb{F}_2 , and also to the propositional clause $v \iff w$. Meanwhile, the inconsistency equation $\sigma(v, w) = -1$ corresponds to $x_v + x_w = 1$, and also to the propositional clause $v \oplus w$, where $\oplus = \text{XOR}$. Therefore, we

7. See, e.g., <https://github.com/mars0i/popco>, https://github.com/russellcameronthomas/JavaECHO_command_line, <https://github.com/B-Sabev/ComputationalModelsOfCoherence>, <https://github.com/tjd/echo>, or <https://github.com/MaxRae/ConnectionistSudoku>. Even the two most recent of these have not been updated for six years as of this writing.

can repackage G_σ into the linear equation $Bx = c$, where B is the incidence matrix of G_σ , or equivalently the biadjacency matrix of the factor graph of the 2-XORSAT/2-Affine-SAT (Roy, 2006; Mezard and Montanari, 2009) formula obtained from the clauses indicated just above.

For example, the coherence graph in Figure 4 corresponds to the linear equation

$$\begin{pmatrix} 1 & 1 & 0 & 0 & 0 \\ 0 & 1 & 1 & 0 & 0 \\ 0 & 1 & 0 & 1 & 0 \\ 0 & 1 & 0 & 0 & 1 \\ 0 & 0 & 1 & 1 & 0 \\ 0 & 0 & 0 & 1 & 1 \\ 1 & 0 & 0 & 0 & 1 \end{pmatrix} \begin{pmatrix} x_a \\ x_b \\ x_c \\ x_d \\ x_e \end{pmatrix} = \begin{pmatrix} 1 \\ 0 \\ 1 \\ 0 \\ 0 \\ 1 \\ 0 \end{pmatrix}$$

and also to the propositional formula

$$(a \oplus b) \wedge (b \iff b) \wedge (b \oplus d) \wedge (b \iff e) \wedge (c \iff d) \wedge (d \oplus e) \wedge (e \iff a).$$

By using the identities $v \iff w \equiv (\neg v \vee w) \wedge (v \vee \neg w)$ and $v \oplus w \equiv (v \vee w) \wedge (\neg v \vee \neg w)$, we can transform this into a CNF-SAT formula.

Of course, in general the linear equation has no solution and the propositional formula is unsatisfiable. In the propositional context, the coherence computation corresponds to the MAX-2-XORSAT problem, which unsurprisingly reduces to MAX-CUT (Moore and Mertens, 2011). To our knowledge, the linear algebra formulation of coherence does not appear in the literature.⁸ The goal is to find a certain approximate solution to $Bx = c$, where again B is the incidence matrix (over \mathbb{F}_2) of G_σ , x is a vector of propositional truth values, and c is a vector encoding σ . Specifically, we want to find the assignment x that satisfies the most rows of the equation: this is equivalent to satisfying the most clauses, i.e., to solving MAX-(2-XOR)SAT all over again. In the language of sparse approximation, we want to solve $\arg \min_x \|Bx - c\|_0$ over \mathbb{F}_2 , where the L^0 “norm” (i.e., the size of the support) is indicated.⁹ We can write this as a more conventional-looking optimization with objective $\sum_j (-1)^{c_j + e_j^T Bx}$ (Jordan et al., 2024). However, there is a more general formulation as an integer linear program (Vazirani, 2001) whose relaxation is of substantial practical interest, as we shall discuss in the sequel.

A.2. A general approach: weighted MAX-SAT

We sketch how to represent higher-order (in)consistency relationships such as trilemmas. A conceptually simple but computationally involved general approach is as follows:

- for each ordered pair of dependent claims, rate the consistency of the second given the first, and associate this to a weight for an implication term;

8. However, this formulation of the MAX-XORSAT problem is found in the literature on low-density generator matrix codes, where it is equivalent to performing source encoding (Wainwright et al., 2010).

9. Note that i) over \mathbb{F}_2 , the L^0 and L^1 norms are the same, but this offers no advantage; and ii) the usual problem of sparse approximation is of the form $\min_y \|y\|_0$ such that $b = Ay$. Our problem is not expressible in this way and it does not appear to be treated in the literature from the perspective of sparse approximation/optimization, cf. (Natarajan, 1995).

- for each ordered triple of dependent claims, rate the consistency of the second and third given the first, and separately the consistency of the third given the first and second: associate these with corresponding implication terms;
- etc., truncating this hierarchy as desired/practical.

Note that this requires a clique-finding algorithm such as that of [Chiba and Nishizeki \(1985\)](#), and that each unordered tuple corresponds to several ordered tuples, ensuring symmetry.

While this approach appears to adequately generalize the notion of a coherence graph into what amounts to a weighted *simplicial complex*—i.e., a weighted hypergraph containing all sub-hyperedges ([Rosiak, 2022](#))—it is not yet suitable for practical MAX-SAT solvers of any sort. These only address weighted CNF-SAT problems, while common translations into CNF-SAT do not preserve weights correctly. Therefore, applying a MAX-SAT solver would generally require (implementing and) applying a specialized transformation of the sort detailed in [Li et al. \(2022\)](#), which to our knowledge has no public implementation.

Once a coherence problem is properly transformed into CNF-SAT, there is an interesting alternative to weighted MAX-SAT solvers. An efficient probabilistic algorithm for weighted MAX-SAT discussed in [Vazirani \(2001\)](#) provides a natural probabilistic interpretation that is certain to be useful in many if not most practical situations. For example, a proposition with acceptance probability near 0.5 may indicate a need for—and even drive the collection of—additional data for incorporation into the relevant structure.

The general approach to representing and solving “higher-order” coherence problems outlined just above was suggested by [Huntsman et al. \(2024\)](#), who were unaware of prior work on coherence *per se*. The underlying motivation was that a *sheaf* ought to represent consistency data. Briefly, a sheaf is comprised of data on open sets in a topological space that satisfy natural restriction—equivalently, gluing—axioms ([Rosiak, 2022](#)). The connection to sheaves is that every logical clause in a CNF-SAT formula introduces a logical constraint that must be satisfied in order for the overall formula to be satisfied. In particular, adding clauses can never enlarge the solution space ([Srinivas, 1993](#)).

It is not immediately clear how to adapt our approach for modeling coherence graphs to this more general setting. We leave this for future work.

Appendix B. A case study comparing human and LLM consistency ratings

There is additional evidence that LLMs can reliably gauge propositional (in)consistency ([Huntsman et al., 2024](#); [Kumar and Roussinov, 2024](#)). However, we are not aware of any assessment of performance relative to humans. Here, we outline a case study performed in summer 2024 in which ChatGPT 4 demonstrated superhuman performance at gauging (in)consistency.

In [Thagard \(1992\)](#), a coherence graph modeled a decision facing the captain of the cruiser USS *Vincennes* on 3 July 1988: was radar track 4131 taking off from the Iranian civilian-military airfield at Bandar Abbas a civilian aircraft, or a hostile F-14 preparing to attack? The coherence graph included “positive evidence” propositions (labeled E*) copied almost verbatim from §III.C.1.b of the investigation report ([Fogarty, 1988](#)) along with a few of their negations (labeled NE*) and hypothetical propositions that the track was attacking (labeled A*) or commercial (labeled C*). As is still common today for analyses using CDI, the edge set and weights (here, simply signs) were constructed by hand.

To focus on ChatGPT 4’s performance in evaluating (in)consistency, we considered the same edge set as the manually-constructed coherence graph, i.e., we neglected any considerations of dependence.

It is important to note here that (the nontrivial connected component of) the coherence graph has $|V| = 21$ and $|E| = 36$, so its edge density is $36/210 = 0.17$. **In other words, this example is in exactly the same regime as the larger and sparser benchmark graphs discussed in the main text.**

For each edge, we asked ChatGPT 4 to rate the consistency of the corresponding pairs of propositions 10 times using a variant of the prompt in [Huntsman et al. \(2024\)](#) that included an extract from the executive summary of [Fogarty \(1988\)](#) as background information. The results are shown in Figures 9 and 10. Supporting data and scripts are in [Huntsman \(2024\)](#).

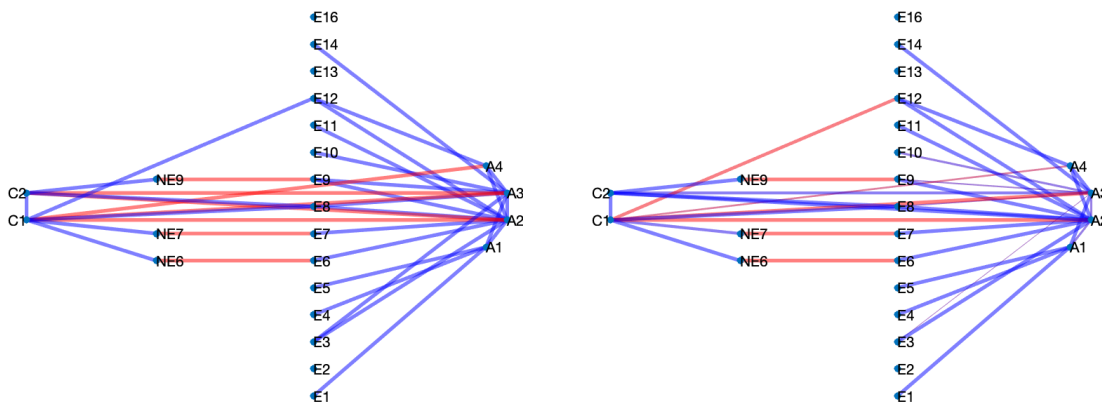


Figure 9: Left: A hand-crafted coherence graph from [Thagard \(1992\)](#). Blue and red respectively indicate positive and negative edge weights. Right: A coherence graph with the same edges, but with weights given by rescaled median consistency ratings from ChatGPT 4. Thickness indicates the relative magnitude of weights.

A bit of introspection and common sense reveals that for the largest discrepancies between the median LLM rating and the human rating, the median LLM rating is more reasonable in each event. Consider the four largest discrepancies, listed in order of their appearance in Figure 10:

A2-C2: These are obviously consistent, so ChatGPT 4’s rating is better than the rating in [Thagard \(1992\)](#).

- A2 is “Track 4131 was an F-14.”
- C2 is “Track 4131 was taking off.”

A3-E3: Examination of outputs shows that ChatGPT 4 considered plausible technical failures and misunderstandings. In light of this, it is fair to conclude that ChatGPT 4’s rating is better than the rating in [Thagard \(1992\)](#).

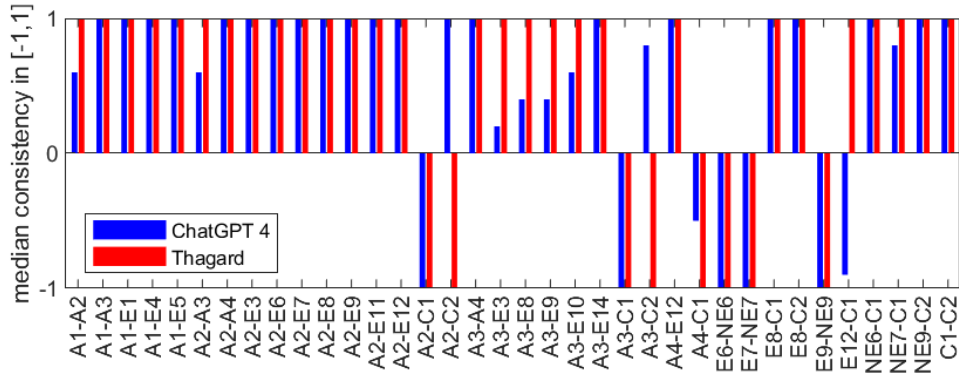


Figure 10: Rescaled median consistency ratings by ChatGPT 4 versus hand-crafted consistency ratings from Thagard (1992).

- A3 is “Track 4131 intended to attack.”
- C3 is “Track 4131 was not responding to verbal warnings over [air distress frequencies].”

A3-C2: Both A3 and C2 are listed above. These are obviously consistent, so ChatGPT 4’s rating is better than the rating in Thagard (1992).

E12-C1: Examination of outputs shows that ChatGPT 4 considered navigation and communications emissions of commercial airliners. In light of this, it is fair to conclude that ChatGPT 4’s rating is better than the rating in Thagard (1992).

- E12 is “No [electronic emissions were reported] from track 4131, however, F-14s can fly [without electronic emissions].”
- C1 is “Track 4131 was a commercial airliner.”

To summarize, ChatGPT 4 demonstrated superhuman performance at gauging the (in)consistency of propositions.

Appendix C. ANOVA for micro F_1

The two-way ANOVA for micro F_1 in Table 1 shows significant effects.

Appendix D. Modeling and reconstruction under uncertainty

D.1. Syntax can model uncertainty in propositions

To evaluate model judgments of consistency under uncertainty, we borrow from Ragin (2006). We introduce uncertainty to p or $\neg p$ by sampling from triangular fuzzy membership functions defined over the unit interval, with 1 and 0 respectively corresponding to p and $\neg p$. After adding uncertainty, a given p -assignment is syntactically represented as something like $0.619 * p$, while a given $\neg p$

	SS	DF	F	p-value
C(model)	17.86	11.0	60.77	< 0.001
density	9.87	1.0	369.50	< 0.001
C(model):density	1.84	11.0	6.28	< 0.001
residual	22.87	856.0	NaN	NaN

Table 1: A two-way ANOVA shows significance for model, sparsity, and their interaction.

assignment is syntactically represented as something like $0.346 * p$. That is, we indicate uncertainty as in the right panels of Figures 6 and 7, with results in Table 2: meanwhile, the prompt in §I echoes this construction. With $p \leftarrow \alpha * p$ and $\neg p \leftarrow \alpha_{\neg} * p$ we delineate three uncertainty regimes. The low regime has $\alpha \in [0.75, 1]$ and $\alpha_{\neg} \in [0, 0.25]$; the medium regime has $\alpha \in [0.625, 0.75]$ and $\alpha_{\neg} \in [0.25, 0.375]$, and the high regime has $\alpha \in [0.5, 0.625]$ and $\alpha_{\neg} \in [0.375, 0.5]$.

Encoding numerical uncertainty in natural language in a way that ensures accurate interpretation is complicated by individual differences in interpretation related to terms such as “approximately,” “certainly,” “about,” “exactly,” etc. (Krisper et al., 2019; Ferson et al., 2015). This presents a challenge for, e.g., communicating risks related to climate change, risks of developing complications from medical treatment, or the likelihood of a given geopolitical event in the future (DNI, 2015). The fuzzy set method above encodes diverse qualitative statements with a consistent formalism, and is directly relevant for use with words of estimative probability (DNI, 2015; Kachynskiy, 2019).

D.2. LLMs successfully infer synthetic coherence graphs under uncertainty

Table 2 shows that introducing uncertainty does not degrade graph reconstruction fidelity.

In Figure 11, we show how recursively passing an inferred uncertain coherence graph to o1-mini and prompting it to assign weights reflective of the level of uncertainty in property assignments can yield a weighted coherence graph with appropriate edge weights (less certain assignments yield smaller magnitude weights; more certain assignments yield larger magnitude weights).

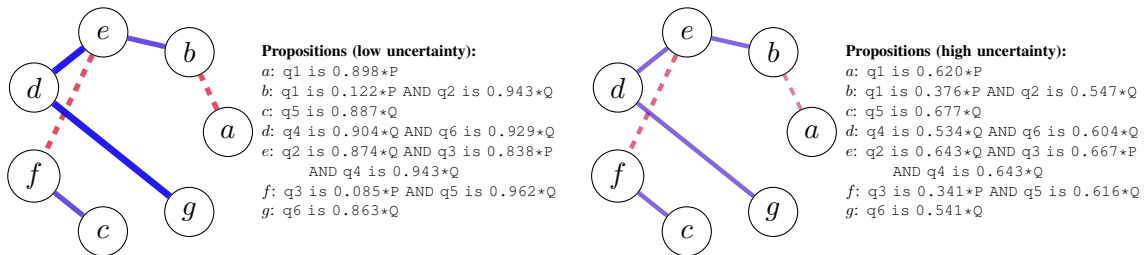


Figure 11: o1-mini-inferred weights have larger magnitude (indicated here by thickness as well as by color and opacity) when uncertainty is lower (as in the left panel). Both left and right panels reflect perfect reconstructions of the underlying graph.

model	sparsity	base case	zero unc.	low unc.	med unc.	high unc.
o1-mini	sparse	0.94 ± 0.10	0.93 ± 0.10	0.93 ± 0.10	0.93 ± 0.10	0.94 ± 0.11
	dense	0.74 ± 0.14	0.71 ± 0.16	0.68 ± 0.16	0.73 ± 0.16	0.75 ± 0.13
o3-mini	sparse	0.97 ± 0.06	0.97 ± 0.07	0.97 ± 0.06	0.97 ± 0.06	0.97 ± 0.06
	dense	0.78 ± 0.10	0.77 ± 0.09	0.79 ± 0.08	0.77 ± 0.08	0.79 ± 0.07
o4-mini	sparse	0.98 ± 0.06	0.98 ± 0.06	0.98 ± 0.06	0.98 ± 0.06	0.98 ± 0.06
	dense	0.79 ± 0.09	0.80 ± 0.07	0.80 ± 0.07	0.80 ± 0.07	0.80 ± 0.07
Gemini 1.5	sparse	0.74 ± 0.18	0.75 ± 0.18	0.77 ± 0.15	0.81 ± 0.13	0.77 ± 0.17
	dense	0.48 ± 0.14	0.48 ± 0.16	0.48 ± 0.13	0.49 ± 0.14	0.48 ± 0.12
Gemini 2.0	sparse	0.71 ± 0.23	0.68 ± 0.23	0.72 ± 0.20	0.73 ± 0.19	0.73 ± 0.22
	dense	0.49 ± 0.13	0.47 ± 0.11	0.46 ± 0.13	0.44 ± 0.10	0.48 ± 0.12
GPT-4o	sparse	0.73 ± 0.19	0.75 ± 0.16	0.74 ± 0.21	0.74 ± 0.18	0.73 ± 0.17
	dense	0.46 ± 0.14	0.43 ± 0.10	0.44 ± 0.14	0.46 ± 0.15	0.44 ± 0.12
Phi-4	sparse	0.53 ± 0.29	0.43 ± 0.31	0.42 ± 0.30	0.41 ± 0.28	0.43 ± 0.24
	dense	0.49 ± 0.13	0.49 ± 0.16	0.47 ± 0.12	0.50 ± 0.16	0.50 ± 0.13
Claude 3.5	sparse	0.92 ± 0.11	0.91 ± 0.13	0.91 ± 0.12	0.91 ± 0.12	0.91 ± 0.11
	dense	0.59 ± 0.15	0.61 ± 0.15	0.59 ± 0.15	0.60 ± 0.14	0.62 ± 0.15
Llama 3.3	sparse	0.54 ± 0.26	0.53 ± 0.26	0.55 ± 0.22	0.62 ± 0.23	0.50 ± 0.26
	dense	0.42 ± 0.16	0.47 ± 0.15	0.43 ± 0.16	0.46 ± 0.16	0.42 ± 0.15
QwQ	sparse	0.92 ± 0.13	0.90 ± 0.14	0.90 ± 0.13	0.91 ± 0.13	0.91 ± 0.13
	dense	0.61 ± 0.19	0.59 ± 0.18	0.59 ± 0.19	0.60 ± 0.20	0.62 ± 0.21
Sky-T1	sparse	0.76 ± 0.18	0.68 ± 0.23	0.62 ± 0.28	0.67 ± 0.21	0.68 ± 0.24
	dense	0.43 ± 0.14	0.43 ± 0.13	0.41 ± 0.14	0.42 ± 0.13	0.43 ± 0.13

Table 2: LLMs successfully infer synthetic coherence graphs under uncertainty (unc).

Appendix E. Benchmark generation parameters can be altered to synthesize problem sets with desired characteristics

Figure 12 demonstrates how benchmark generation parameters lead to increasing numbers of variables in the resulting synthetic problem sets as graph sizes increase. The top row shows data for small graphs (5-11 propositions), middle row: medium graphs (13-17 propositions), bottom row: large graphs (19-23 propositions). In general, the `degenerate` edge clique processing method and the `partition` method (first and third subcolumns in each panel) lead to more variables and fewer properties than the `percolation` method (middle column of each panel).

Appendix F. Inferring logical entailment with ModernBERT fine-tuned for NLI

We performed a preliminary experiment to test whether we could directly identify either a) relevance (defined as two propositions sharing a single variable) or b) consistency directly from white box LLM embeddings or from a number of simple quantifications of inter-token attention in the models’ attention mechanisms. While these experiments showed a consistently high error rate (suggesting the need for a more sophisticated mechanistic interpretability study along the lines described by Nanda et al. 2023) we report the best results, which came from using a small BERT model (ModernBERT fine-tuned to infer entailment relations between propositions (Sileo, 2024; Reimers and Gurevych, 2019)).

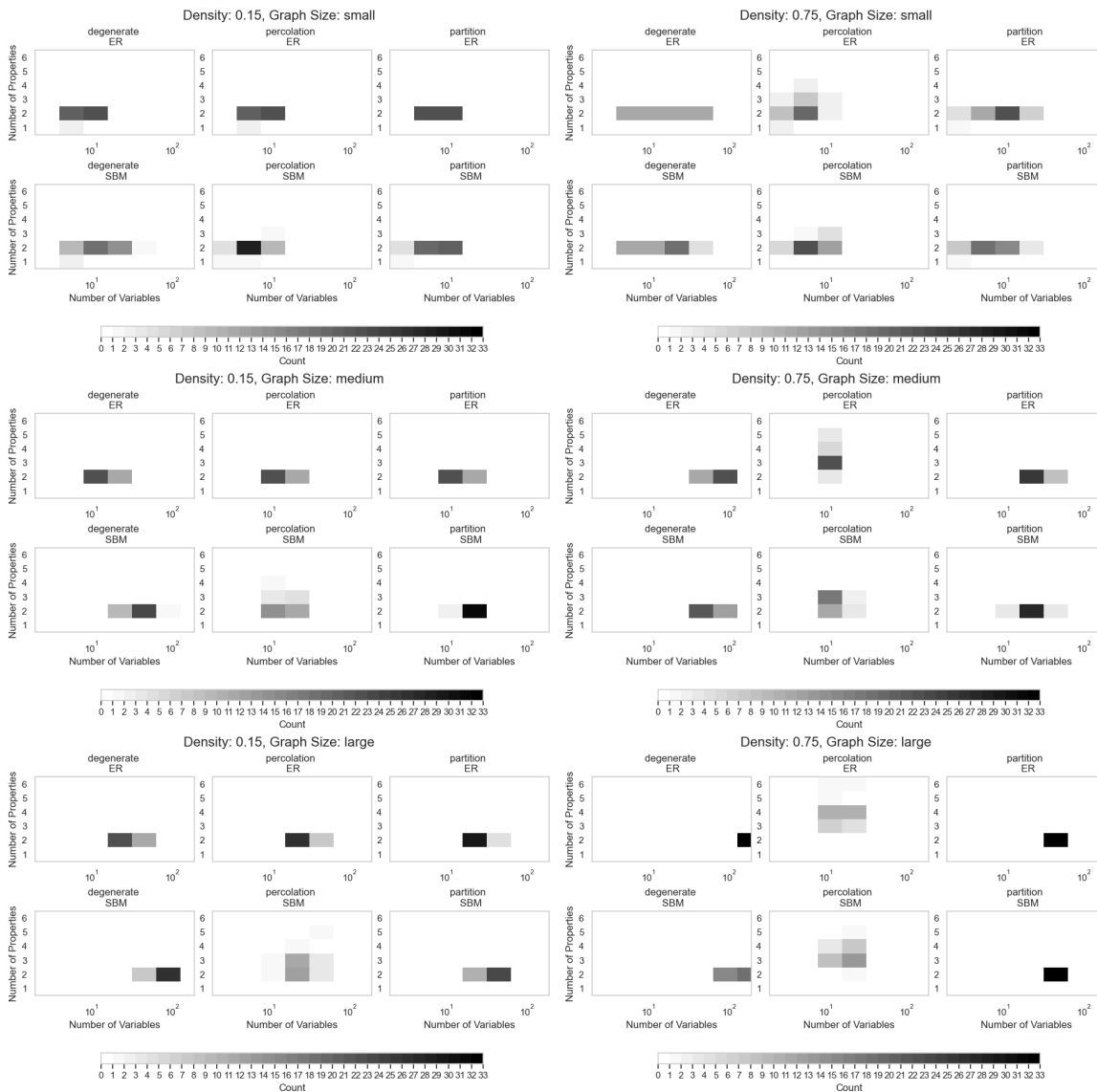


Figure 12: Figure 12 Changing benchmark generation parameters leads to increasing numbers of variables in the resulting synthetic problem sets as graph sizes increase. Top row: small graphs (5-11 propositions). Middle row: medium graphs (13-17 propositions). Bottom row: large graphs (19-23 props). In general, the degenerate edge clique processing method and the partition method (first and third subcolumns in each panel) lead to more variables and fewer properties than the percolation method (middle column of each panel).

Using propositions in the simplified natural language grammar of our benchmark shows accurate entailment inferences along the diagonal (left figure), but multiple errors in off-diagonal relations (e.g., inferring a contradiction in (2,4) between "q₂ is !P" and "q₄ is !P", among others). However, rewriting propositions more formally (right) shows that `ModernBERT` is able to perfectly infer consistency relations among these propositions.

Our tests to extract logical relations directly from attention encodings included estimating e.g., mean or median inter-token attention at the first layer, last layer, or across all layers for `QwQ-32B` (the most performant open source LLM for our purposes) using benchmark propositions and propositions rewritten in propositional logic. We also tested applying regression to correct positional and autoregressive attention effects. These experiments were inconclusive, suggesting that more complex statistical measures might be needed to identify reasoning mechanisms in white box models.

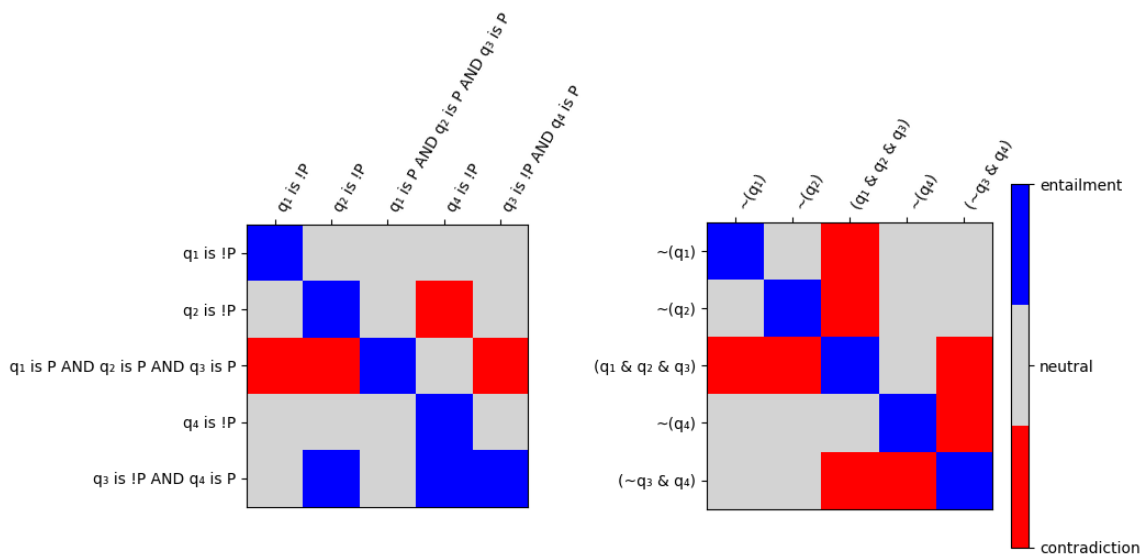


Figure 13: Pairwise natural language inference using `ModernBERT` for propositions of a simple one property problem shows errors on benchmark propositions (left) but perfect accuracy with propositions transformed to propositional logic (right).

Appendix G. Characteristics of synthetic coherence graphs included in our benchmark experiment

In Table 3, we show that our experiment includes coherence graphs ranging in size from 5 to 23 propositions. We note that our requirement that all synthetic coherence graphs be connected makes harder to meet the desired sparsity (*sparse* and *dense* corresponding to target densities of 0.15 and 0.75 respectively) levels for smaller graphs (5-11 propositions).

n propositions	sparsity	n variables median	n properties median	edges median	density mean	problem count
5	sparse	4.0	1.5	4.0	0.400000	4
	dense	3.0	2.0	7.0	0.700000	4
7	sparse	6.0	2.0	6.0	0.285714	4
	dense	5.5	2.0	15.0	0.714286	4
9	sparse	8.0	2.0	8.0	0.222222	4
	dense	6.5	2.0	27.0	0.750000	4
11	sparse	10.0	2.0	10.0	0.181818	4
	dense	9.5	3.0	41.0	0.745455	4
13	sparse	12.0	2.0	12.0	0.153846	4
	dense	13.5	2.0	58.0	0.743590	4
15	sparse	15.0	2.0	15.0	0.142857	4
	dense	17.5	2.5	78.0	0.742857	4
17	sparse	19.0	2.0	20.0	0.147059	4
	dense	23.0	2.5	102.0	0.750000	4
19	sparse	22.0	2.0	25.0	0.146199	4
	dense	29.0	2.5	128.0	0.748538	4
21	sparse	27.0	2.0	31.0	0.147619	3
	dense	42.0	2.0	157.0	0.747619	3
23	sparse	32.0	2.0	37.0	0.146245	3
	dense	52.0	2.0	189.0	0.747036	3

Table 3: Our experimental benchmark includes 76 graphs (N=38 *sparse* and N=38 *dense*) ranging in size from 5 to 23 propositions.

Appendix H. L^1 /graph edit distance convergence

Figure 14 shows how taking a median of multiple coherence graphs can yield a stable, broadly reproducible result.

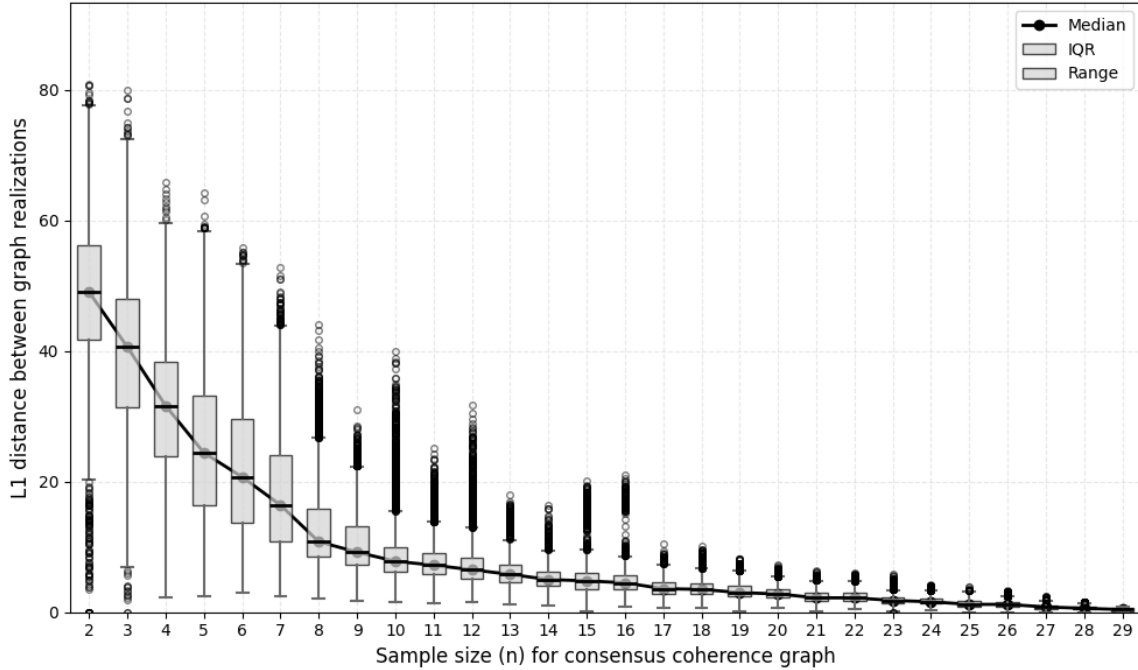


Figure 14: L^1 /graph edit distance between medians of n of $N = 30$ coherence graphs used to construct the consensus of N coherence graphs in Figure 2. This sort of convergence is typical but not ubiquitous.

Appendix I. Prompt for global consistency inference under uncertainty

We show an example of the prompt used as a template for all inference attempts in Table I.

Appendix J. Prompt for practical examples

The prompt we used for practical examples such as shown in Figures 2 and 3 is in Table J. It evolved from prompts used since spring 2023 to determine models' ability to evaluate the pairwise consistency of propositions [Huntsman et al. \(2024\)](#).

Appendix K. Fidelity of the reconstruction of the graph measured by the L^1 norm normalized by graph size

The reconstruction of a coherence graph G_σ is automatically of the form $G'_{\sigma'}$, where $V(G_\sigma) = V(G'_{\sigma'})$. Therefore, it is easy and appropriate to use the metric $d(G_\sigma, G'_{\sigma'}) := \|A(G_\sigma) - A(G'_{\sigma'})\|_1$,

For the input set of propositions, identify which propositions are logically consistent (i.e., can coexist without contradiction). Construct a networkx graph where inconsistent edges are weight 1 and consistent edges are weight 0. If two vertices do not involve the same variables, do not create an edge between them.

Return solely the edge list with proposition names for vertices. i.e., return responses in this format:

```
[('b', 'c', 0),
 ('b', 'e', 0),
 ('c', 'd', 0),
 ('c', 'e', 0)]
```

Variables:

```
['q1', 'q2', 'q3', 'q4']
```

A given variable can have these properties:

```
property P: P XOR !P
property Q: Q XOR !Q
property R: R XOR !R
property S: S XOR !S
```

A given property is assigned in a fuzzy manner:

```
property 1: !P := < 0.5P. P := ≥ 0.5P
property 2: !Q := < 0.5Q. Q := ≥ 0.5Q
property 3: !R := < 0.5R. R := ≥ 0.5R
property 4: !S := < 0.5S. S := ≥ 0.5S
```

Input:

```
['Proposition(a): "q1 is !P"',
 'Proposition(b): "q2 is !P"',
 'Proposition(c): "q1 is P AND q2 is P AND q3 is P"',
 'Proposition(d): "q4 is !P"',
 'Proposition(e): "q3 is !P AND q4 is P"']
```

Table 4: Prompt for global consistency inference

where adjacency matrices are indicated, and we permit $A(\cdot) \in [-1, 1]$ here for the sake of generality. This coincides with a graph edit distance in which edge insertion and deletion costs are the absolute value of the edge weight, and in which edge substitution costs are the absolute value of the difference of edge weights. Normalizing this by $|V| \cdot (|V| - 1)/2$ gives a size-independent gauge of performance.

Figure 15 shows that o1/3/4-mini, claude-3.5-sonnet and QwQ-32B-Preview outperform all other models on sparse problems using this measure of adjacency matrix similarity to characterize reconstruction error.

Imagine that you are a perfectly objective arbitrator with impeccable judgment and integrity. In response to a prompt of the form 'buildCoherence: ' below followed by a list of labeled propositions, please do the following: First, determine which pairs of propositions are substantively related. Second, for each related pair of propositions, determine their logical relationship, assuming that at least one is true, whether or not either actually is. I want you to ignore the truth, falsity or basis in fact of either claim. Third, based on your determination just above, numerically rate the relative consistency of the two propositions. Do not pay attention to or comment on the truth or basis in fact of either proposition independent of the other. Your rating of relative consistency should be on a scale from 0 to 10, with a value of 0 for a pair of propositions that are not at all consistent and a value of 10 for a pair of propositions that are totally consistent. I cannot emphasize enough that for your rating, I want you to ignore the truth or basis in fact of either proposition, since anything that is not consistent with reality cannot be true. If you determine that propositions are unrelated despite previously determining otherwise, omit that pair. To be clear, a pair of false but consistent claims should also be rated a 10. Meanwhile, a pair of propositions of which one is true and the other is false, should be rated a 0. Finally, construct a NetworkX graph where propositions are vertices and edges correspond to substantively related pairs of propositions, with weights given by the consistency ratings just above. Only return the edge list with proposition labels for vertices. i.e., return responses in this format (here 'p2', 'p3', 'p4', and 'p5' are labels): [('p2', 'p3', 0), ('p2', 'p5', 10), ('p3', 'p4', 9), ('p3', 'p5', 2)]. Order vertices (in edges) and edges (in the graph) lexicographically.

buildCoherence:

Table 5: Prompt for practical examples

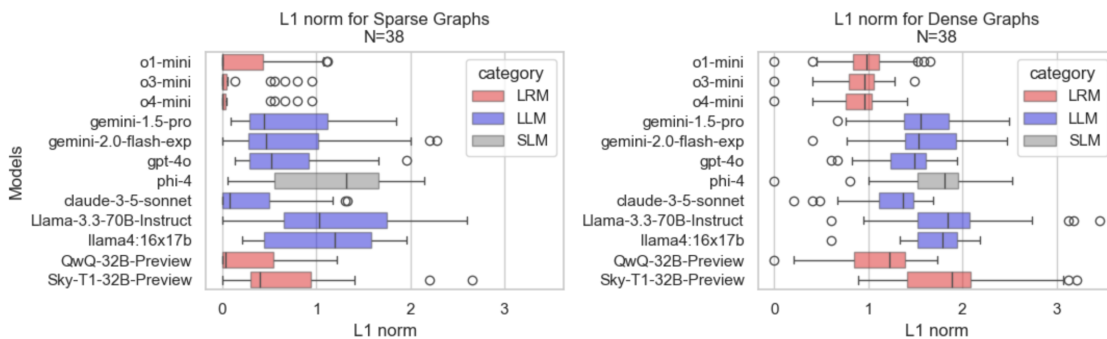


Figure 15: o1/3/4-mini, claude-3.5-sonnet, and QwQ-32B have lower (higher fidelity) L_1 scores than other models.

